CLEAVAGE OF 4-NITROPHENYL DIPHENYL PHOSPHATE BY ISOMERIC QUATERNARY PYRIDINIUM KETOXIMES – HOW CAN STRUCTURE AND LIPOPHILICITY OF FUNCTIONAL SURFACTANTS INFLUENCE THEIR REACTIVITY IN MICELLES AND MICROEMULSIONS?

Milan KIVALA[1], Radek CIBULKA[2] and František HAMPL[3,*]

Department of Organic Chemistry, Institute of Chemical Technology, Prague, Technická 5, 166 28 Prague 6, Czech Republic; e-mail: [1] kivala@org.chem.ethz.ch, [2] cibulkar@vscht.cz, [3] hamplf@vscht.cz

Received October 10, 2006
Accepted December 1, 2006

Amphiphilic pyridinium ketoximes 4-[1-(hydroxyimino)alkyl]-1-methylpyridinium bromides (**1**) and 1-alkyl-4-[1-(hydroxyimino)ethyl]pyridinium bromides (**2**) are isomeric cationic surfactants bearing the nucleophilic hydroxyimino group. They differ in the position of the nucleophilic function relative to polar head group and hydrophobic alkyl chain. The 4-nitrophenyl diphenyl phosphate (PNPDPP) cleavage by the oximate anions generated from **1** and **2** was used as a model reaction for the investigation of the influence of the structure and lipophilicity of functional surfactants on their reactivity in micelles and microemulsions. The investigation of the model reaction in cationic micelles of hexadecyltrimethylammonium bromide (CTAB), in non-ionic micelles (Triton X-100 and Brij 35) and in o/w microemulsion (isooctane/phosphate buffer/CTAB and butan-1-ol) has revealed that it is the lipophilicity which is the most important factor influencing the localization and reactivity of functional surfactants in nanoaggregates.

Keywords: Functional surfactants; Micelles; Microemulsions; Nanoaggregates; Pyridinium oximes; Phosphate esters cleavage.

In the recent decades, various aspects of reactivity of functional surfactants in micelles, vesicles, and microemulsions have been investigated and discussed in hundreds or rather thousands of papers and in many books and reviews[1]. Colloids containing various types of functional surfactants and metallosurfactants have often been considered as enzyme mimics. Among them, models of hydrolases seem to be of considerable interest. Possible applications, particularly hydrolysis of neurotoxic derivatives of phosphoric and phosphonic acid have stimulated extensive research in this area[2]. Much effort has been spent on attempts to increase the efficiency of hydrolytic catalysts based on micelles, vesicles, and microemulsions con-

Collect. Czech. Chem. Commun. 2006, Vol. 71, Nos. 11–12, pp. 1642–1658

doi:10.1135/cccc20061642

taining reactive functional surfactants. The research has been focused predominantly on the reactive function design[1d,1f] and on optimization of colloid system properties[1d,1f]. Less attention has been paid to relative position and orientation of the reactants in micelles and vesicles despite the fact that the restricted mobility of amphiphilic molecules (both translational and rotational) can dramatically influence their reactivity in these nanoaggregates. Only a few studies have explored the relation between the reactivity of functional surfactants and probable location and orientation of their reactive function in the nanoaggregate arising from the surfactant molecule shape, i.e. from relative position of its polar head group, hydrophobic alkyl chain and reactive function. For example, Ogino and coworkers[3] investigated the hydrolytic activity of two types of imidazole-based metallosurfactants in hexadecyltrimethylammonium bromide (CTAB) and sodium dodecyl sulfate (SDS) micelles. In the former type, the charged group terminated the hydrophobic chain and the functional group (2-(hydroxymethyl)imidazole moiety coordinated to Cu^{2+}) was inside the surfactant molecule while in the latter the functional group was terminal and a charged group inside. Another example is a series of studies performed by Romsted and coworkers[4] who utilized amphiphilic arenediazonium salts as probes for the estimation of distribution of the anions around cationic micelles. The structures of the probes employed in these experiments were designed to allow them to take up the desired position of the reactive diazonium function at the micelle/aqueous phase interface.

As a part of our research oriented to design of potential micellar catalysts for hydrolysis of organophosphates, we have synthesized several amphiphilic quaternary pyridinium ketoximes and examined their efficiency in hydrolysis of 4-nitrophenyl diphenyl phosphate[5] (PNPDPP) which is one of the most frequently used models of organophosphate nerve agents. Due to its lipophilicity it is reasonable to assume that PNPDPP is almost completely solubilized in micellar core. The results of kinetic measurements of the PNPDPP hydrolysis in various micellar and metallomicellar systems[6] were in accord with this assumption. We have found that the reactivity of isomeric pyridinium ketoximes **1c** and **2c** depends on the position of their nucleophilic hydroxyimino function relative to polar head group and hydrophobic alkyl chain[5a]. Thus, the apparent second-order rate constant k_2 of the PNPDPP cleavage by the oximate anion formed from ketoxime **1c** is higher than that of the reaction with the anion formed from its isomer **2c**. We have concluded that the observed higher reactivity of the isomer **1c** ensues from the fact that its nucleophilic hydroxyimino group is located be-

low the micellar surface thus increasing the probability of the lipophilic substrate attack as shown in an idealized chart (Fig. 1).

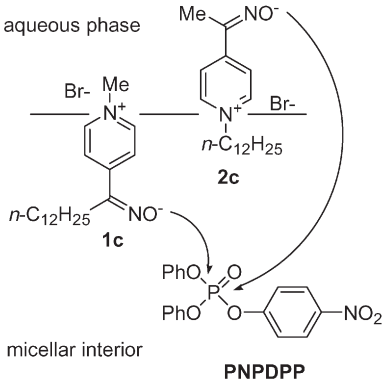

FIG. 1
Orientation of molecules of surfactants **1c** and **2c** at micelle/aqueous phase interface

High efficiency of the PNPDPP cleavage by amphiphilic ketoximes **1c** and **2c** in cationic micelles of CTAB as well as an interesting relationship between their structure and reactivity to PNPDPP prompted us to extend the preliminary study to homologous ketoximes **1** and **2** with the hydrophobic alkyls C8–C16, thus covering the interval of log *P* values approximately from 1.5 to almost 6, and to other nanoaggregates such as non-ionic micelles and o/w microemulsion (partition coefficient *P* between octan-1-ol and water was used as a generally accepted measure of lipophilicity). We assumed that the comparison of the reactivity of both series of isomeric ketoximes **1** and **2** towards PNPDPP in various colloid systems should permit us to make some general conclusion as far as the structure of the functional surfactant and its orientation at the interface of the nanoaggregate is concerned. From the point of view of possible applications, the finding of

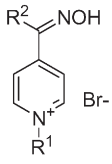

	R^1	R^2
1a	Me	*n*-C_8H_{17}
1b	Me	*n*-$C_{10}H_{21}$
1c	Me	*n*-$C_{12}H_{25}$
1d	Me	*n*-$C_{16}H_{33}$
2a	*n*-C_8H_{17}	Me
2b	*n*-$C_{10}H_{21}$	Me
2c	*n*-$C_{12}H_{25}$	Me
2d	*n*-$C_{16}H_{33}$	Me

the optimum type of the colloid system for hydrolysis of organophosphates catalyzed by ketoximes **1** and **2** was expected. Just as in our preliminary study[5a], PNPDPP was used as a model substrate with well defined localization in colloid systems.

RESULTS AND DISCUSSION

*Synthesis of Quaternary Pyridinium Ketoximes **1** and **2***

4-[1-(Hydroxyimino)alkyl]-1-methylpyridinium bromides **1** were prepared analogously to the previously described synthetic route[5b] with the following exceptions: (i) instead of a Grignard reagent, the corresponding alkyllithium was used in the preparation of ketones **3a**, **3b**, and **3d**, (ii) 4-[1-(hydroxyimino)alkyl]-1-methylpyridinium bromides **1** were prepared directly by quaternization of the corresponding alkyl pyridin-4-yl ketoxime **4** with methyl bromide (Scheme 1). 1-Alkyl-4-[1-(hydroxyimino)ethyl]pyridinium bromides **2** were obtained by quaternization of methyl 4-pyridinyl ketoxime (prepared from commercial 4-acetylpyridine and hydroxylamine) with the corresponding alkyl bromides.

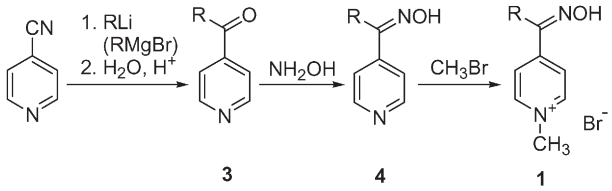

SCHEME 1

Configuration at C=N bond of methyl pyridin-4-yl ketoxime and oxime **4d** was assigned by NOE experiments. Irradiation of H^2 or H^3 aromatic protons affords NOE transferred to proton of the hydroxyimino group (Fig. 2a) and, furthermore, irradiation of the proton of hydroxyimino group affords NOE to both H^2 and H^3 aromatic protons thus giving evidence of *Z* configuration. We did not observe NOE between α-methylene protons of the alkyl chain and proton of the hydroxyimino group which should be expected for (*E*)-isomers (Fig. 2b). In the case of all other alkyl pyridin-4-yl ketoximes **4**, *Z* configurations was assigned as well since the corresponding heteroaromatic protons shifts were practically the same as in the case of **4d** and methyl pyridin-4-yl ketoxime. It is known that chemical shifts of heteroaromatic protons in alkyl pyridinyl ketoximes are strongly influenced by the C=N bond configuration – the differences in chemical shifts of the cor-

responding heteroaromatic protons in (*E*)- and (*Z*)-isomers are up to 0.28 ppm [7]. The results of NOE experiments allowed us to correct the erroneous assignment of the configuration in alkyl pyridin-4-yl ketoximes stated in our previous communication[5b] which was done on the basis of the empirical Roberts rule[8]. All the prepared quaternary salts **1** and **2** were of uniform configuration since only one set of signals was found in their ^{1}H and ^{13}C NMR spectra. We assume that their configuration is *Z* as well since the isomerization of the hydroxyimino group is hardly probable under the reaction conditions of quaternization. The log *P* values of PNPDPP and ketoximes **1** and **2** were calculated using a software package Pallas 1.2 (ref.[9]).

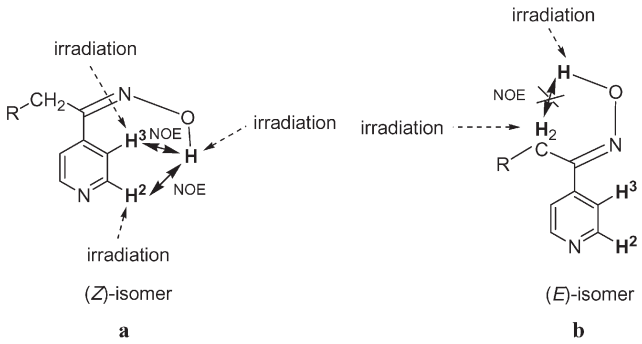

FIG. 2
NOE interactions in alkyl pyridin-4-yl ketoximes: (*Z*)-isomer (a), (*E*)-isomer (b)

Micellar Solutions and o/w Microemulsions

Cationic surfactant CTAB and non-ionic surfactants Triton X-100 and Brij 35 are the most frequently used amphiphiles for the preparation of micellar systems for various kinetic studies[1] and therefore we chose them for our experiments as well. The resulting concentration of these non-reactive "inert" surfactants in the prepared micellar solutions (1.0×10^{-2} mol l^{-1}) sufficiently exceeded those of functional surfactants **1** or **2**, which ranged from 2.5×10^{-4} to 2.5×10^{-3} mol l^{-1}. Therefore we assumed that the properties of micellar matrices in the corresponding series of experiments were comparable being determined by the inert surfactant.

The o/w microemulsion type used in our experiments was inspired by Bhattacharya[10a]. He performed kinetic studies of ester hydrolysis catalyzed by lipophilic supernucleophiles in microemulsions representing pseudoternary systems consisting of phosphate buffer (water), cyclohexane (oil) and

CTAB with butan-1-ol which served as a co-surfactant. In our experiments, we replaced cyclohexane with less volatile isooctane. As a "surfactant" component, we employed the 1:1 mixture (weight ratio) of CTAB and butan-1-ol and phosphate buffer (0.1 mol l^{-1}, pH 7.0) was used as "water". The pseudo-ternary system behaviour was investigated point-by-point by titration of the phosphate buffer–surfactant mixtures with isooctane. Each composition marked in the diagram in Fig. 3 represents a clear liquid of low viscosity, isotropic in polarized light, of long-term stability. Since the phosphate buffer was a major component, we classified these microemulsions as o/w. As evident from Fig. 3, there exists a relatively large area of compositions in which this pseudoternary system forms stable o/w microemulsions.

A question arose which composition from the area shown in Fig. 3 is optimal from the point of view of the maximum rate of the PNPDPP cleavage by ketoximes **1** and **2**. Since a regular three-parameter optimization of the microemulsion composition seemed to be beyond the scope of this work we chose the composition only on the basis of the considerations given below. It was reasonable to assume that the concentration of reactants in the oil phase (and, consequently, also the observed reaction rate) is inversely proportional to the isooctane content in microemulsion[10]. On the other hand, the influence of the surfactant content was not evident at the first sight.

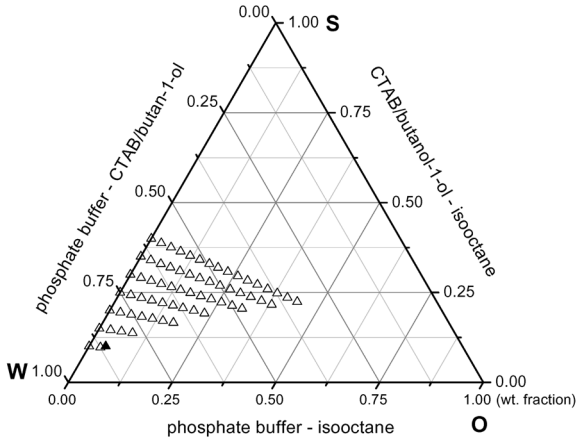

FIG. 3

Pseudoternary system oil (isooctane)–water (0.1 M phosphate buffer, pH 7.0)–surfactant (CTAB/butan-1-ol 1:1) with the area of o/w microemulsion (△). Composition used for kinetic experiments (▲). Outside the marked area either heterogeneous systems or lyotropic liquid–crystalline phases were found

Therefore, we have measured the dependence of the pseudo-first-order rate constant k_{obs} of the PNPDPP cleavage by ketoximes **1** and **2** on the surfactant content in microemulsion (Fig. 4). The isooctane content (4%) was kept constant in these experiments. The obtained data have revealed that the observed reactivity of ketoximes **1** and **2** towards PNPDPP is inversely proportional to the surfactant content in microemulsion as well. Thus, the maximum reaction rate can be expected if both the oil and the surfactant content are suppressed to minimum. These findings led us to choose the following microemulsion composition: isooctane (4%), phosphate buffer pH 7.0 (86%), CTAB (5%) and butan-1-ol (5%).

*Reactivity of Ketoximes **1** and **2** in Micellar Solutions and o/w Microemulsions*

It is well recognized that the regression analysis of absorbance (or any other macroscopic quantity giving evidence of the reaction course) vs time data affords the apparent rate constant only, which is an average value calculated for the total reaction system volume if the reaction is carried out in heterogeneous systems. Therefore, the apparent second-order rate constant k_2 values correspond to real reaction rates neither in micellar pseudophase nor in microemulsion oil phase where the local molarities of lipophilic re-

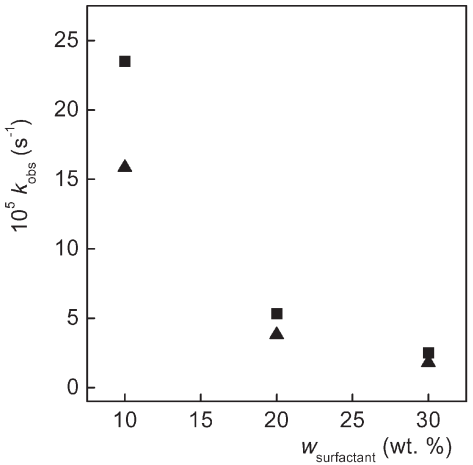

FIG. 4
Dependence of the pseudo-first-order rate constant k_{obs} of the PNPDPP cleavage by ketoximes **1** (■) and **2** (▲) on the surfactant (CTAB/1-butanol 1:1) content in microemulsions containing 4% of isooctane. Conditions: [**1**] = [**2**] = 1.0×10^{-3} mol l^{-1}, [PNPDPP] = 2.0×10^{-5} mol l^{-1}, T = 25 °C

actants are substantially higher compared with analytical (average) concentrations[11]. Nevertheless, this particular fact brings the advantage of implicit information on the concentration of reactants in colloid particles and on other circumstances influencing the reaction rate such as availability of the reactants and their relative orientation in colloid particles.

The obtained results of the PNPDPP cleavage by ketoximes **1** and **2** in micelles and o/w microemulsion are summarized in Fig. 5. Regardless of the type of micellar system, the reactivity of both types of pyridinium ketoximes increases with their lipophilicity. This trend is not surprising since more lipophilic compounds are more tightly bound by the nanoaggregates[1a,12]. According to generally accepted opinion[12,13], cationic micelles increase the rate of alkaline hydrolysis due to the positive charge of the micellar surface which increases the local pH value. Indeed, the reactivity of ketoximes **1** and **2** in CTAB micelles was the highest in the investigated systems.

The observed reactivity of ketoximes **1** and **2** in o/w microemulsions is much lower compared with micellar solutions. This fact is not surprising since the concentrations of the reactants in oil phases of microemulsions are usually lower compared with those in micellar phase[10]. Micellar phase in 1.0×10^{-2} M CTAB makes ca. 0.4% of the total solution volume involving the assumption that molar volume of micellized CTAB in aqueous solutions

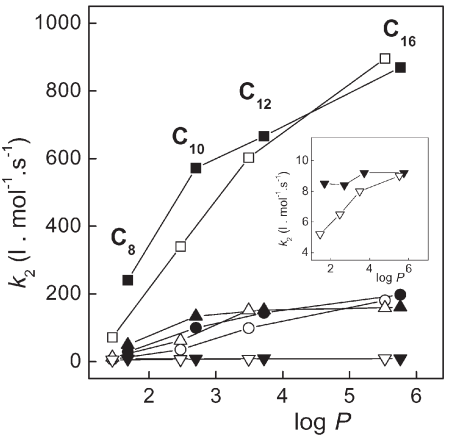

FIG. 5

Dependence of the second-order rate constant k_2 of the PNPDPP cleavage by ketoximes **1** (full symbols) and **2** (open symbols) on their lipophilicity (log *P*) in different types of aggregates: CTAB (■, □), Triton X-100 (●, ○), Brij 35 (▲, △), and o/w microemulsion (▼, ▽). The lines help the eyes to follow the data points.

is 0.37 l mol^{-1} (ref.[14]). On the other hand, in microemulsions employed in our kinetic experiments the oil phase fraction made ca. 6% of the total volume.

The reactivity of ketoximes **2** in o/w microemulsion increases with their lipophilicity although this trend is much less pronounced compared with micellar solutions. The reactivity of ketoximes **1** is practically unaffected by their lipophilicity. We assume that a higher proportion of the organic phase in o/w microemulsions increases the efficiency of the extraction of ketoximes **1** and **2** into colloid particles in comparison with micelles thus diminishing the effect of increasing lipophilicity.

At first sight, the influence of the structure of ketoximes **1** and **2** on their reactivity in micelles and o/w microemulsion is not obvious from the second-order rate constants k_2 values given in Fig. 5. A better information on the behaviour of isomeric ketoximes **1** and **2** in nanoaggregates affords comparison of the reactivity of the corresponding homologues (Fig. 6). On going from C8 to C16 homologues, the ratio of second-order rate constants $(k_2)_\mathbf{1}/(k_2)_\mathbf{2}$ for ketoximes **1** and **2** of the same hydrophobic alkyl chain length (and practically the same lipophilicity) decreases in all types of the examined nanoaggregates converging to unity for C16. In other words, the difference in the reactivity of both isomeric ketoximes **1** and **2** practically disappears in the case of sufficiently lipophilic homologues.

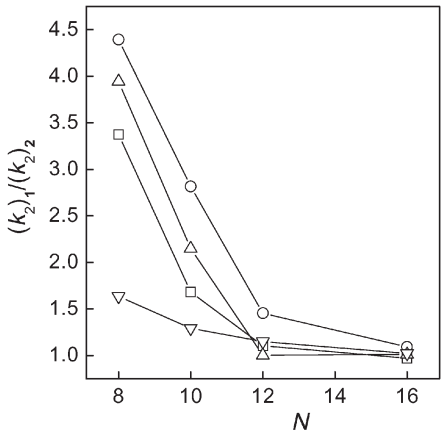

FIG. 6

Dependence of the ratio of second-order rate constants $(k_2)_\mathbf{1}/(k_2)_\mathbf{2}$ for the corresponding homologues of ketoximes **1** and **2** on the hydrophobic alkyl chain length in various types of aggregates: CTAB (□), Triton X-100 (○), Brij 35 (△), and o/w microemulsion (▽). The lines help the eyes to follow the data points

Most likely, less lipophilic ketoximes **1** and **2** prefer to set at the boundary of the nanoaggregate with the orientation depicted in Fig. 1 as reported previously[5a]. On the other hand, more lipophilic surfactants (log P > 4 in this particular case) are prone, regardless of their structure, to leave the interface and react in the interior of the nanoaggregate. Thus, contrary to our previous hypothesis[5a], the lipophilicity of the functional surfactant seems to be a more important factor influencing its reactivity in any micellar system investigated than its structure i.e. mutual position of the polar head group, hydrophobic alkyl chain and functional group. As shown in an idealized chart in Fig. 7, the influence of lipophilicity is even capable to overcome the influence of the structure differences in the case of isomeric functional surfactants **1** and **2**. The close resemblance of the plots of the relative reactivity of ketoximes **1** and **2** in micelles vs hydrophobic chain length (Fig. 6) supports this hypothesis. The discussed behavior observed in micelles is less pronounced in the o/w microemulsion for the reasons mentioned above.

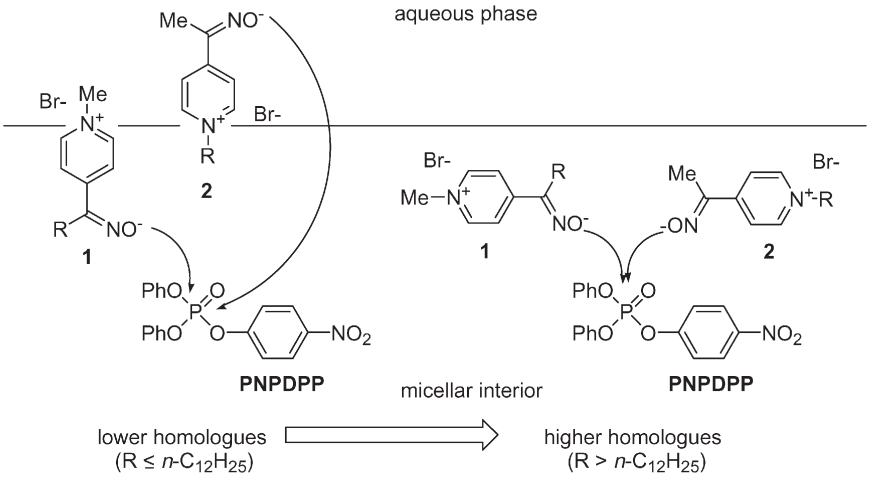

FIG. 7
Schematic illustration explaining the reactivity of amphiphilic ketoximes **1** and **2** in nanoaggregates

Conclusion

Although examined in the case of isomeric pyridinium ketoximes **1** and **2** only, it is reasonable to assume that the above discussed principles are applicable to assessment of the reactivity of any functional surfactant in nanoaggregates and should be taken into consideration in the design of any micellar catalyst and optimization of its efficiency.

EXPERIMENTAL

General

Melting points were uncorrected. ^{1}H and ^{13}C NMR spectra were recorded on a Varian Gemini 300 (operating at 300.1 and 75.1 MHz for ^{1}H and ^{13}C, respectively) or on a Bruker AMX3 400 (operating at 400.1 and 100.6 MHz for ^{1}H and ^{13}C, respectively). Chemical shifts (δ, ppm) are reported relative to internal Me_4Si. All coupling constants (*J*) are in Hz. TLC analyses were carried out on DC Alufolien Kieselgel 60 F254. Preparative column chromatography was performed on silica gel 60, 0.040–0.063 mm.

Chemicals

All the chemicals used in the syntheses (quality purum or pract.) were used as received. The solvents were purified and dried according to described procedures[15]. Hexadecyltrimethylammonium bromide (CTAB) puriss., isooctane for HPLC (not less than 99.5%), and Brij 35 were obtained from Aldrich, Triton X-100 from Fluka. Butan-1-ol and other chemicals and materials (puriss.) were supplied by Lachema. 4-Nitrophenyl diphenyl phosphate (PNPDPP) was prepared and purified according to the described procedure[16]. The o/w microemulsion for the kinetic experiments was prepared by vigorous mixing of a mixture of 0.1 M phosphate buffer, pH 7.0 (86 wt.%), isooctane (4 wt.%), CTAB (5 wt.%), and butan-1-ol (5 wt.%) at ambient temperature. The resulting o/w microemulsion (clear liquid of low viscosity, isotropic in polarized light, pH 7.0) was stable for months.

Alkyl Pyridin-4-yl Ketones **3**. General Procedure

A solution of alkyllithium[17] (ca. 0.2 mol l^{-1}; 0.091 mol) in ether or a 1 M solution of dodecylmagnesium bromide in ether was added dropwise at –30 °C to a solution of pyridine-4-carbonitrile (0.091 mol) in ether (450 ml) within 1 h. After 1 h stirring at –10 °C and warming-up to room temperature the reaction mixture was quenched with 2 M hydrochloride acid. pH of the mixture was adjusted to 8 with potassium carbonate. The organic layer was separated, the aqueous solution was extracted with ether (5 × 150 ml) and the combined organic layers were dried with anhydrous magnesium sulfate. Evaporation of the solvent afforded crude product which was purified by column chromatography (chloroform–methanol 100:3).

Octyl pyridin-4-yl ketone (**3a**). Yield 72.2%. White crystals, m.p. 37.5–39 °C. ^{1}H NMR ($CDCl_3$): 0.81 t, 3 H, *J*(8′,7′) = 6.6 (CH_3); 1.21 bs, 10 H ($(CH_2)_5$); 1.67 tt, 2 H, *J*(2′,1′) = *J*(2′,3′) = 7.3 (C**H**$_2$CH$_2$C=O); 2.89 t, 2 H, *J*(1′,2′) = 7.3 (CH_2C=O); 7.65 dd, 2 H, *J*(3,2) = *J*(5,6) = 4.4,

J(3,5) = *J*(5,3) = 1.5 (H-3, H-5); 8.73 d, 2 H, *J*(2,3) = *J*(6,5) = 5.3 (H-2, H-6). ^{13}C NMR ($CDCl_3$): 14.3 s (CH_3); 22.9 s (CH_2CH_3); 24.1 s ($CH_2CH_2CH_3$); 29.5 t ($(CH_2)_3$); 32.0 s (CH_2CH_2C=O); 39.1 s (CH_2C=O); 121.3 s (C-3, C-5); 143.1 s (C-4); 151.2 s (C-2, C-6); 200.1 s (C=O). For $C_{14}H_{21}NO$ (219.3) calculated: 76.67% C, 9.65% H, 6.39% N; found: 76.62% C, 10.29% H, 6.33% N.

Decyl pyridin-4-yl ketone (**3b**). Yield 92.9%. White crystals, m.p. 51–52.5 °C. ^{1}H NMR ($CDCl_3$): 0.81 t, 3 H, *J*(10′,9′) = 6.6 (CH_3); 1.20 bs, 14 H ($(CH_2)_7$); 1.66 tt, 2 H, *J*(2′,1′) = *J*(2′,3′) = 7.3 (C**H**$_2$CH$_2$C=O); 2.89 t, 2 H, *J*(1′,2′) = 7.3 (CH_2C=O); 7.65 dd, 2 H, *J*(3,2) = *J*(5,6) = 4.4, *J*(3,5) = *J*(5,3) = 1.7 (H-3, H-5); 8.73 dd, 2 H, *J*(2,3) = *J*(6,5) = 4.4, *J*(2,6) = *J*(6,2) = 1.7 (H-2, H-6). ^{13}C NMR ($CDCl_3$): 14.3 s (CH_3); 22.9 s (CH_2CH_3); 24.1 s ($CH_2CH_2CH_3$); 29.6 m ($(CH_2)_5$); 32.1 s (CH_2CH_2C=O); 39.1 s (CH_2C=O); 121.3 s (C-3, C-5); 143.1 s (C-4); 151.2 s (C-2, C-6); 200.1 s (C=O). For $C_{16}H_{25}NO$ (247.4) calculated: 77.68% C, 10.19% H, 5.66% N; found: 77.38% C, 10.20% H, 5.60% N.

Dodecyl pyridin-4-yl ketone (**3c**). Yield 66.5%. White crystals, m.p. 55–60 °C (ref.[5b] 56–60 °C). ^{1}H NMR ($CDCl_3$): 0.87 t, 3 H, *J*(12′,11′) = 6.7 (CH_3); 1.25 bs, 18 H ($(CH_2)_9$); 1.73 tt, 2 H, *J*(2′,1′) = *J*(2′,3′) = 7.3 (C**H**$_2$CH$_2$C=O); 2.95 t, 2 H, *J*(1′,2′) = 7.3 (CH_2C=O); 7.72 dd, 2 H, *J*(3,2) = *J*(5,6) = 4.4, *J*(3,5) = *J*(5,3) = 1.8 (H-3, H-5); 8.80 dd, 2 H, *J*(2,3) = *J*(6,5) = 4.4, *J*(2,6) = *J*(6,2) = 1.8 (H-2, H-6). ^{13}C NMR ($CDCl_3$): 14.3 s (CH_3); 22.9 s (CH_2CH_3); 24.1 s ($CH_2CH_2CH_3$); 29.7 m ($(CH_2)_7$); 32.1 s (CH_2CH_2C=O); 39.1 s (CH_2C=O); 121.3 s (C-3, C-5); 143.1 s (C-4); 151.2 s (C-2, C-6); 200.1 s (C=O). For $C_{18}H_{29}NO$ (275.4) calculated: 78.49% C, 10.61% H, 5.09% N; found: 78.23% C, 10.49% H, 4.90% N.

Hexadecyl pyridin-4-yl ketone (**3d**). Yield 78.5%. White crystals, m.p. 71–75 °C. ^{1}H NMR ($CDCl_3$): 0.87 t, 3 H, *J*(16′,15′) = 6.6 (CH_3); 1.28 bs, 26 H ($(CH_2)_{13}$); 1.73 tt, 2 H, *J*(2′,1′) = *J*(2′,3′) = 7.3 (C**H**$_2$CH$_2$C=O); 2.95 t, 2 H, *J*(1′,2′) = 7.3 (CH_2C=O); 7.72 dd, 2 H, *J*(3,2) = *J*(5,6) = 4.5, *J*(3,5) = *J*(5,3) = 1.5 (H-3, H-5); 8.80 dd, 2 H, *J*(2,3) = *J*(6,5) = 4.5, *J*(2,6) = *J*(6,2) = 1.5 (H-2, H-6). ^{13}C NMR ($CDCl_3$): 14.3 s (CH_3); 22.9 s (CH_2CH_3); 24.1 s ($CH_2CH_2CH_3$); 29.7 m ($(CH_2)_{11}$); 32.1 s (CH_2CH_2C=O); 39.1 s (CH_2C=O); 121.3 s (C-3, C-5); 143.0 s (C-4); 151.2 s (C-2, C-6); 200.0 s (C=O). For $C_{22}H_{37}NO$ (331.6) calculated: 79.70% C, 11.25% H, 4.22% N; found: 80.03% C, 11.60% H, 4.10% N.

Alkyl Pyridin-4-yl Ketoximes **4**. General Procedure

Aqueous solution of hydroxylamine (50%; 0.329 mol) was added in two portions to the boiling solution of ketone **3** (0.065 mol) in methanol (200 ml) within 14 h. Evaporation of solvent gave crude product, which was purified by column chromatography (chloroform–methanol 100:6). The described procedure afforded almost pure (>95%) (*Z*)-isomers of **4a** and **4b**. In the case of ketoximes **4c** and **4d**, the *Z*/*E* ratio was 11:1 and 9:1, respectively. Pure (*Z*)-**4c** and (*Z*)-**4d** were obtained by crystallization from aqueous ethanol.

(Z)-Octyl pyridin-4-yl ketoxime (**4a**). Yield 80.5%. White crystals, m.p. 85–90 °C. ^{1}H NMR ($CDCl_3$): 0.86 t, 3 H, *J*(8′,7′) = 6.2 (CH_3); 1.25 bs, 10 H ($(CH_2)_5$); 1.56 tt, 2 H, *J*(2′,1′) = *J*(2′,3′) = 7.4 (C**H**$_2$CH$_2$C=O); 2.80 t, 2 H, *J*(1′,2′) = 7.3 (CH_2C=O); 7.59 dd, 2 H, *J*(3,2) = *J*(5,6) = 4.7, *J*(3,5) = *J*(5,3) = 1.4 (H-3, H-5); 8.64 dd, 2 H, *J*(2,3) = *J*(6,5) = 4.7, *J*(2,6) = *J*(6,2) = 1.7 (H-2, H-6); 11.75 s, 1 H (OH). ^{13}C NMR ($CDCl_3$): 14.3 s (CH_3); 22.9 s (CH_2CH_3); 25.5 s ($CH_2CH_2CH_3$); 26.5 s ($CH_2(CH_2)_2CH_3$); 29.5 d ($(CH_2)_2$); 30.1 s (CH_2CH_2C=NOH); 32.0 s (CH_2C=NOH); 120.9 s (C-3, C-5); 144.4 s (C-4); 149.9 s (C-2, C-6); 157.2 s (C=NOH). For $C_{14}H_{22}N_2O$ (234.3) calculated: 71.76% C, 9.46% H, 11.95% N; found: 72.40% C, 9.69% H, 12.03% N.

(Z)-Decyl pyridin-4-yl ketoxime (**4b**). Yield 65.4%. White crystals, m.p. 88–91.5 °C. ^{1}H NMR ($CDCl_3$): 0.80 t, 3 H, J(10′,9′) = 6.5 (CH_3); 1.22 bs, 14 H ((CH_2)$_7$); 1.49 tt, 2 H, J(2′,1′) = J(2′,3′) = 7.3 (C**H**$_2$CH$_2$C=NOH); 2.72 t, 2 H, J(1′,2′) = 7.9 (C**H**$_2$C=NOH); 7.65 d, 2 H, J(3,2) = J(5,6) = 6.1 (H-3, H-5); 8.57 d, 2 H, J(2,3) = J(6,5) = 6.2 (H-2, H-6); 9.77 s, 1 H (OH). ^{13}C NMR ($CDCl_3$): 14.3 s (CH_3); 22.9 s (C**H**$_2$CH$_3$); 25.5 s (C**H**$_2$CH$_2$CH$_3$); 26.5 s (C**H**$_2$(CH$_2$)$_2$CH$_3$); 29.7 m ((CH$_2$)$_4$); 30.0 s, (C**H**$_2$CH$_2$C=NOH); 32.1 s (C**H**$_2$C=NOH); 120.9 s (C-3, C-5); 144.3 s (C-4); 149.9 s (C-2, C-6); 157.6 s (C=NOH). For $C_{16}H_{26}N_2O$ (262.4) calculated: 73.24% C, 9.99% H, 10.68% N; found: 73.27% C, 10.06% H, 10.59% N.

(Z)-Dodecyl pyridin-4-yl ketoxime (**4c**). Yield 73.8%. White crystals, m.p. 91–95 °C (ref.[5b] 92–94 °C). ^{1}H NMR ($CDCl_3$): 0.87 t, 3 H, J(12′,11′) = 6.5 (CH_3); 1.24 bs, 18 H ((CH_2)$_9$); 1.55 tt, 2 H, J(2′,1′) = J(2′,3′) = 7.7 (C**H**$_2$CH$_2$C=NOH); 2.78 t, 2 H, J(1′,2′) = 7.9 (C**H**$_2$C=NOH); 7.54 dd, 2 H, J(3,2) = J(5,6) = 5.4, J(3,5) = J(5,3) = 0.9 (H-3, H-5); 8.63 d, 2 H, J(2,3) = J(6,5) = 6.2 (H-2, H-6); 10.25 s, 1 H (OH). ^{13}C NMR ($CDCl_3$): 14.3 s (CH_3); 22.9 s (C**H**$_2$CH$_3$); 25.5 s (C**H**$_2$CH$_2$CH$_3$); 26.0 s (C**H**$_2$(CH$_2$)$_2$CH$_3$); 26.5 s (C**H**$_2$(CH$_2$)$_3$CH$_3$); 29.8 m ((CH$_2$)$_5$); 32.1 s (C**H**$_2$CH$_2$C=NOH); 33.0 s (C**H**$_2$C=NOH); 120.8 s (C-3, C-5); 144.3 s (C-4); 150.0 s (C-2, C-6); 157.4 s (C=NOH). For $C_{18}H_{30}N_2O$ (290.5) calculated: 74.44% C, 10.41% H, 9.64% N; found: 74.15% C, 10.58% H, 9.52% N.

(Z)-Hexadecyl pyridin-4-yl ketoxime (**4d**). Yield 84.4%. White crystals, m.p. 94–96.5 °C. ^{1}H NMR ($CDCl_3$): 0.87 t, 3 H, J(16′,15′) = 6.7 (CH_3); 1.24 bs, 26 H ((CH_2)$_{13}$); 1.55 tt, 2 H, J(2′,1′) = J(2′,3′) = 7.5 (C**H**$_2$CH$_2$C=NOH); 2.78 t, 2 H, J(1′,2′) = 7.7 (C**H**$_2$C=NOH); 7.53 dd, 2 H, J(3,2) = J(5,6) = 4.9, J(3,5) = J(5,3) = 1.4 (H-3, H-5); 8.63 dd, 2 H, J(2,3) = J(6,5) = 4.8, J(2,6) = J(6,2) = 1.4 (H-2, H-6); 9.09 s, 1 H (OH). ^{13}C NMR ($CDCl_3$): 14.3 s (CH_3); 22.9 s (C**H**$_2$CH$_3$); 25.5 s (C**H**$_2$CH$_2$CH$_3$); 26.5 s (C**H**$_2$(CH$_2$)$_2$CH$_3$); 29.8 m ((CH$_2$)$_{11}$); 32.1 s (C**H**$_2$C=NOH); 120.8 s (C-3, C-5); 143.9 s (C-4); 150.2 s (C-2, C-6); 157.9 s (C=NOH). For $C_{22}H_{38}N_2O$ (346.6) calculated: 76.25% C, 11.05% H, 8.08% N; found: 76.18% C, 11.33% H, 7.80% N.

4-[1-(Hydroxyimino)alkyl]-1-methylpyridinium Bromides **1**. General Procedure

A solution of oxime **4** (0.047 mol) and methyl bromide (0.5 mol) in methanol (100 ml) was stirred at 45 °C for 15 h under a cold-finger reflux condenser cooled with ethanol–CO_2(s). Then, the solvent with the unreacted methyl bromide were evaporated and the remaining crude product was purified by column chromatography (chloroform–methanol–acetone–water 15:5:5:1) followed by crystallization from the mixture acetone–diethyl ether. All the prepared quaternary oximes were of uniform configuration since only one set of signals was found in their ^{1}H or ^{13}C NMR spectra. It is evident that the configuration of the quaternary salts **1** is the same as in oximes **4**.

4-[1-(Hydroxyimino)nonyl]-1-methylpyridinium bromide (**1a**). Yield 69.2%. M.p. 147–151 °C. ^{1}H NMR (DMSO-d_6): 0.82 t, 3 H, J(8′,7′) = 6.6 (CH_3); 1.20 bs, 10 H ((CH_2)$_5$); 1.40 m, 2 H (C**H**$_2$CH$_2$C=NOH); 2.78 t, 2 H, J(1′,2′) = 7.4 (C**H**$_2$C=NOH); 4.29 s, 3 H (CH_3-N$^+$); 8.26 d, 2 H, J(3,2) = J(5,6) = 6.6 (H-3, H-5); 8.90 d, 2 H, J(2,3) = J(6,5) = 6.8 (H-2, H-6); 12.59 s, 1 H (OH). ^{13}C NMR (DMSO-d_6): 14.6 s (CH_3); 22.7 s (C**H**$_2$CH$_3$); 24.5 s (C**H**$_2$CH$_2$CH$_3$); 26.1 s (C**H**$_2$(CH$_2$)$_2$CH$_3$); 29.3 d ((CH$_2$)$_2$); 29.7 s (C**H**$_2$CH$_2$C=NOH); 31.9 s (C**H**$_2$C=NOH); 48.0 s (CH_3-N$^+$); 123.9 s (C-3, C-5); 146.3 (C-2, C-6); 151.2 s (C-4); 154.7 s (C=NOH). For $C_{15}H_{25}BrN_2O$ (329.3) calculated: 54.71% C, 7.65% H, 8.51% N; found: 54.66% C, 8.26% H, 8.69% N.

4-[1-(Hydroxyimino)undecyl]-1-methylpyridinium bromide (**1b**). Yield 70.7%. M.p. 134–137 °C. ^{1}H NMR (DMSO-d_6): 0.82 t, 3 H, J(10′,9′) = 6.7 (CH_3); 1.20 bs, 10 H ((CH_2)$_5$); 1.40 m, 2 H (C**H**$_2$CH$_2$C=NOH); 2.78 t, 2 H, J(1′,2′) = 7.6 (C**H**$_2$C=NOH); 4.31 s, 3 H (CH_3-N$^+$); 8.26 d, 2 H, J(3,2) = J(5,6) = 6.9 (H-3, H-5); 8.93 d, 2 H, J(2,3) = J(6,5) = 6.6 (H-2, H-6); 12.56 s, 1 H (OH). ^{13}C NMR (DMSO-d_6): 14.6 s (CH_3); 22.8 s (C**H**$_2$CH$_3$); 24.5 s (C**H**$_2$CH$_2$CH$_3$); 26.2 s (C**H**$_2$(CH$_2$)$_2$CH$_3$); 29.5 m ((CH_2)$_5$); 32.0 s (C**H**$_2$C=NOH); 48.0 s (CH_3-N$^+$); 123.9 s (C-3, C-5); 146.3 s (C-2, C-6); 151.1 s (C-4); 154.7 s (C=NOH). For $C_{17}H_{29}BrN_2O$ (357.3) calculated: 57.14% C, 8.18% H, 7.84% N; found: 57.11% C, 8.25% H, 7.88% N.

4-[1-(Hydroxyimino)tridecyl]-1-methylpyridinium bromide (**1c**). Yield 53.5%. M.p. 122–125 °C. ^{1}H NMR (DMSO-d_6): 0.82 t, 3 H, J(12′,11′) = 6.6 (CH_3); 1.20 bs, 18 H ((CH_2)$_9$); 1.40 m, 2 H (C**H**$_2$CH$_2$C=NOH); 2.78 t, 2 H, J(1′,2′) = 7.4 (C**H**$_2$C=NOH); 4.30 s, 3 H (CH_3-N$^+$); 8.26 d, 2 H, J(3,2) = J(5,6) = 6.9 (H-3, H-5); 8.92 d, 2 H, J(2,3) = J(6,5) = 6.9 (H-2, H-6); 12.59 s, 1 H (OH). ^{13}C NMR (DMSO-d_6): 14.6 s (CH_3); 22.8 s (C**H**$_2$CH$_3$); 24.5 s (C**H**$_2$CH$_2$CH$_3$); 26.2 s (C**H**$_2$(CH$_2$)$_2$CH$_3$); 29.5 m ((CH_2)$_7$); 32.0 s (C**H**$_2$C=NOH); 48.0 s (CH_3-N$^+$); 123.9 s (C-3, C-5); 146.3 s (C-2, C-6); 151.2 s (C- 4); 154.7 s (C=NOH). For $C_{19}H_{33}BrN_2O$ (385.4) calculated: 59.22% C, 8.63% H, 7.27% N; found: 59.01% C, 8.65% H, 7.00% N.

4-[1-(Hydroxyimino)heptadecyl]-1-methylpyridinium bromide (**1d**). Yield 68.1%. M.p. 124–126 °C. ^{1}H NMR (DMSO-d_6): 0.82 t, 3 H, J(16′,15′) = 6.3 (CH_3); 1.20 bs, 26 H ((CH_2)$_{13}$); 1.40 m, 2 H (C**H**$_2$CH$_2$C=NOH); 2.78 t, 2 H, J(1′,2′) = 7.4 (C**H**$_2$C=NOH); 4.30 s, 3 H (CH_3-N$^+$); 8.26 d, 2 H, J(3,2) = J(5,6) = 6.6 (H-3, H-5); 8.91 d, 2 H, J(2,3) = J(6,5) = 6.6 (H-2, H-6); 12.60 s, 1 H (OH). ^{13}C NMR (DMSO-d_6): 14.6 s (CH_3); 22.8 s (C**H**$_2$CH$_3$); 24.5 s (C**H**$_2$CH$_2$CH$_3$); 26.2 s (C**H**$_2$(CH$_2$)$_2$CH$_3$); 29.6 m ((CH_2)$_{11}$); 32.0 s (C**H**$_2$C=NOH); 48.0 s (CH_3-N$^+$); 123.9 s (C-3, C-5); 146.3 s (C-2, C-6); 151.2 s (C-4); 154.7 s (C=NOH). For $C_{23}H_{41}BrN_2O$ (441.5) calculated: 62.57% C, 9.36% H, 6.35% N; found: 63.21% C, 9.67% H, 6.11% N.

1-Alkyl-4-[1-(hydroxyimino)ethyl]pyridinium Bromides **2**. General Procedure

A solution of methyl pyridin-4-yl ketoxime (0.073 mol) and alkyl bromide (0.110 mol) in ethanol (200 ml) was refluxed until the conversion of oxime was complete (TLC: chloroform–methanol 5:1). After solvent evaporation, the crude product was purified by column chromatography (chloroform–methanol–acetone–water 15:5:5:1) and by crystallization from a mixture acetone–diethyl ether. All the prepared quaternary oximes were of uniform *Z* configuration since only one set of signals was found in their ^{1}H or ^{13}C NMR spectra.

4-[1-(Hydroxyimino)ethyl]-1-octylpyridinium bromide (**2a**). Reaction time 37 h. Yield 65.4%. M.p. 132–136 °C. ^{1}H NMR (DMSO-d_6): 0.81 t, 3 H, J(8′,7′) = 6.3 (CH_3); 1.22 bs, 10 H ((CH_2)$_5$); 1.87 m, 2 H (C**H**$_2$CH$_2$N$^+$); 2.22 s, 3 H (CH_3-C=N); 4.58 t, 2 H, J(1′,2′) = 7.4 (CH_2N^+); 8.28 d, 2 H, J(3,2) = J(5,6) = 6.9 (H-3, H-5); 9.08 d, 2 H, J(2,3) = J(6,5) = 6.9 (H-2, H-6); 12.65 s, 1 H (OH). ^{13}C NMR (DMSO-d_6): 11.5 s (C**H**$_3$-C=NOH); 14.6 s (CH_3); 22.7 s (C**H**$_2$CH$_3$); 26.1 s (C**H**$_2$CH$_2$CH$_3$); 29.1 d ((CH_2)$_2$); 31.4 s (C**H**$_2$CH$_2$CH$_2$N$^+$); 31.8 s (C**H**$_2$CH$_2$N$^+$); 60.6 s (CH_2N^+); 124.1 s (C-3, C-5); 145.3 s (C-2, C-6); 151.1 s (C-4); 152.1 s (C=NOH). For $C_{15}H_{25}BrN_2O$ (329.3) calculated: 54.71% C, 7.65% H, 8.51% N; found: 54.67% C, 8.09% H, 8.78% N.

1-Decyl-4-[1-(hydroxyimino)ethyl]pyridinium bromide (**2b**). Reaction time 40 h. Yield 69.8%. M.p. 125.5–127 °C. ^{1}H NMR (DMSO-d_6): 0.82 t, 3 H, J(10′,9′) = 6.3 (CH_3); 1.22 bs, 14 H ((CH_2)$_7$); 1.87 m, 2 H (C**H**$_2$CH$_2$N$^+$); 2.22 s, 3 H (CH_3-C=N); 4.58 t, 2 H, J(1′,2′) = 7.3 (CH_2N^+); 8.28 d, 2 H, J(3,2) = J(5,6) = 6.6 (H-3, H-5); 9.07 d, 2 H, J(2,3) = J(6,5) = 6.6 (H-2, H-6); 12.54 s, 1 H (OH). ^{13}C NMR (DMSO-d_6): 11.5 s (C**H**$_3$-C=NOH); 14.6 s (CH_3); 22.8 s (C**H**$_2$CH$_3$); 26.0 s (C**H**$_2$CH$_2$CH$_3$); 29.1 s (C**H**$_2$(CH$_2$)$_2$CH$_3$); 29.4 t ((CH_2)$_3$); 31.4 s

($CH_2CH_2CH_2N^+$); 31.9 s ($CH_2CH_2N^+$); 60.6 s (CH_2N^+); 124.1 s (C-3, C-5); 145.3 s (C-2, C-6); 151.1 s (C-4); 152.1 s (C=NOH). For $C_{17}H_{29}BrN_2O$ (357.3) calculated: 57.14% C, 8.18% H, 7.84% N; found: 56.67% C, 7.56% H, 7.34% N.

1-Dodecyl-4-[1-(hydroxyimino)ethyl]pyridinium bromide (**2c**). Reaction time 42 h. Yield 72.0%. M.p. 133–134.5 °C (ref.[5b] 128–131 °C). ^{1}H NMR (DMSO-d_6): 0.82 t, 3 H, J(12′,11′) = 6.7 (CH_3); 1.21 bs, 18 H ((CH_2)$_9$); 1.87 m, 2 H ($CH_2CH_2N^+$); 2.22 s, 3 H (CH_3-C=N); 4.57 t, 2 H, J(1′,2′) = 7.3 (CH_2N^+); 8.28 d, 2 H, J(3,2) = J(5,6) = 6.9 (H-3, H-5); 9.06 d, 2 H, J(2,3) = J(6,5) = 6.9 (H-2, H-6); 12.66 s, 1 H (OH). ^{13}C NMR (DMSO-d_6): 11.5 s (CH_3-C=NOH); 14.6 s (CH_3); 22.8 s (CH_2CH_3); 26.1 s ($CH_2CH_2CH_3$); 29.1 s ($CH_2(CH_2)_2CH_3$); 29.5 m ((CH_2)$_5$); 31.4 s ($CH_2CH_2CH_2N^+$); 32.0 s ($CH_2CH_2N^+$); 60.6 s (CH_2N^+); 124.1 s (C-3, C-5); 145.3 s (C-2, C-6); 151.1 s (C-4); 152.1 s (C=NOH). For $C_{19}H_{33}BrN_2O$ (385.4) calculated: 59.22% C, 8.63% H, 7.27% N; found: 58.67% C, 8.61% H, 7.04% N.

1-Hexadecyl-4-[1-(hydroxyimino)ethyl]pyridinium bromide (**2d**). Reaction time 40 h. Yield 63.3%. M.p. 130–134 °C. ^{1}H NMR (DMSO-d_6): 0.82 t, 3 H, J(16′,15′) = 6.6 (CH_3); 1.20 bs, 26 H ((CH_2)$_{13}$); 1.87 m, 2 H ($CH_2CH_2N^+$); 2.22 s, 3 H (CH_3-C=N); 4.55 t, 2 H, J(1′,2′) = 7.3 (CH_2N^+); 8.28 d, 2 H, J(3,2) = J(5,6) = 6.9 (H-3, H-5); 9.03 d, 2 H, J(2,3) = J(6,5) = 6.9 (H-2, H-6); 12.70 s, 1 H (OH). ^{13}C NMR (DMSO-d_6): 11.5 s (CH_3-C=NOH); 14.6 s (CH_3); 22.8 s (CH_2CH_3); 26.1 s ($CH_2CH_2CH_3$); 29.1 s ($CH_2(CH_2)_2CH_3$); 29.6 m ((CH_2)$_9$); 31.4 s ($CH_2CH_2CH_2N^+$); 32.0 s ($CH_2CH_2N^+$); 60.7 s (CH_2N^+); 124.1 s (C-3, C-5); 145.3 s (C-2, C-6); 151.1 s (C-4); 152.1 s (C=NOH). For $C_{23}H_{41}BrN_2O$ (441.5) calculated: 62.57% C, 9.36% H, 6.35% N; found: 61.88% C, 9.68% H, 6.34% N.

Kinetic Measurements

The reactions were performed under pseudo-first-order conditions ($c_{oxime} >> c_{PNPDPP}$) at 25 °C and pH 7.0 (0.1 M phosphate buffer) and their course was monitored with a Hewlett–Packard HP8452 spectrophotometer equipped with a thermostatted multicell transport cell holder HP89075C at 400 nm (absorption maximum of the released 4-nitrophenoxide).

In the case of the reactions performed in micellar solutions, the reaction mixtures were prepared in 1-cm spectrophotometric cells by mixing appropriate volumes of 5.0×10^{-3} M buffered solution of ketoxime **1** or **2**, 2.0×10^{-2} M solution of a micelle-forming surfactant, buffer, and redistilled water. The resulting concentration of the surfactants (CTAB, Triton X-100, Brij 35) was 1.0×10^{-2} mol l^{-1}. The reactions were initiated by injection of 2.0×10^{-3} M PNPDPP solution in acetonitrile (20 μl) into the spectrophotometric cell containing 1980 μl of the buffered micellar solution, the resulting concentration of the substrate being 2.0×10^{-5} mol l^{-1}.

The reactions in o/w microemulsion were performed analogously. The reaction mixtures (1980 μl) were prepared by mixing appropriate volumes of 5.0×10^{-2} M solution of ketoxime **1** or **2** in microemulsion and neat microemulsion. The reactions were initiated by injection of 2.0×10^{-3} M PNPDPP solution in acetonitrile (20 μl) into the spectrophotometric cell.

No changes in pH were observed during kinetic runs. The reactions followed a first-order kinetics at least up to 95% conversion. The pseudo-first-order rate constants k_{obs} were obtained by non-linear regression analysis of the absorbance vs time data using the equation $A_t = (A_{inf} - A_0)\,[1 - \exp(-kt)] + A_0$. Regression analysis was performed using programme Origin 6.1 (ref.[18]). In all cases, the correlation coefficient $r > 0.999$. The kinetic runs were performed in duplicate; the difference in the rate constants did not exceed 5%.

As published elsewhere[5,19], it is the deprotonated hydroxyimino group in pyridinium oximes which is the nucleophile attacking the ester function. Therefore, the apparent second-order rate constants k_2 were obtained as slopes of the pseudo-first-order rate constant k_{obs} of the PNPDPP cleavage vs oximate anion concentration plots; the oximate anion concentrations $c_{oximate}$ at pH 7.0 were calculated from analytical concentrations c_{oxime} and the corresponding pK_a values using the equation $c_{oximate} = c_{oxime}\, K_a/(K_a + [H^+])$.

The authors thank Prof. K. Holmberg, Chalmers University of Technology Göteborg, for the know-how concerning the preparation and treatment of microemulsions and for helpful discussion. This study was supported by Czech Science Foundation, grant No. 203/04/0488.

REFERENCES

1. a) Fendler J. H., Fendler E. J.: *Catalysis in Micellar and Macromolecular Systems*, Chap. 5. Academic Press, New York 1975; b) Fendler J. H.: *Membrane Mimetic Chemistry*, Chap. 12. Wiley, New York 1982; c) Tonellato U. in: *Solution Chemistry of Surfactants* (K. L. Mittal, Ed.), Vol. 2, p. 541. Plenum Press, New York 1979; d) Feiters M. C. in: *Comprehensive Supramolecular Chemistry* (D. N. Reinhoudt, Ed.), Vol. 10, p. 311. Elsevier, Amsterdam 1996; e) Savelli G., Germani R., Brinchi L.: *Surf. Sci. Ser.* **2001**, *100*, 175; f) Oehme G. in: *Aqueous-Phase Organometallic Catalysis* (B. Cornils and W. A. Herrmann, Eds), p. 193. Wiley-VCH, Weinheim 2004.
2. a) Benschop H. P., De Jong L. P. A.: *Acc. Chem. Res.* **1988**, *21*, 368; b) Yang Y.-C., Baker J. A., Ward J. R.: *Chem. Rev.* **1992**, *92*, 1729; c) Yang Y.-C.: *Acc. Chem. Res.* **1999**, *32*, 109; d) Morales-Rojas H., Moss R. A.: *Chem. Rev.* **2002**, *102*, 2497.
3. a) Ogino K., Yoshida T., Nishi K., Fujita T., Tagaki W.: *Chem. Lett.* **1991**, 341; b) Ogino K., Yoshida T., Yamamoto H., Tagaki W.: *Chem. Lett.* **1992**, 1197.
4. a) Romsted L. S., Yao J. H.: *Langmuir* **1999**, *15*, 326; b) Soldi V., Keiper J., Romsted L. S., Cuccovia I. M., Chaimovich H.: *Langmuir* **2000**, *16*, 59; c) Yao J. H., Romsted L. S.: *Langmuir* **2000**, *16*, 8771; d) Menger F. M., Keiper J. S., Mbadugha B. N. A., Caran K. L., Romsted L. S.: *Langmuir* **2000**, *16*, 9095.
5. a) Kotoučová H., Cibulka R., Hampl F., Liška F.: *J. Mol. Catal. A* **2001**, *174*, 59; b) Cibulka R., Hampl F., Kotoučová H., Mazáč J., Liška F.: *Collect. Czech. Chem. Commun.* **2000**, *65*, 227.
6. a) Scrimin P., Tecilla P., Tonellato U.: *J. Org. Chem.* **1991**, *56*, 161; b) Scrimin P., Ghirlanda G., Tecilla P., Moss R. A.: *Langmuir* **1996**, *12*, 6235; c) Bunton C. A., Scrimin P., Tecilla P.: *J. Chem. Soc., Perkin Trans. 2* **1996**, 419.
7. Holzer W., von Philipsborn W.: *Magn. Reson. Chem.* **1989**, *27*, 511.
8. Hawkes G. E., Herwig K., Roberts J. D.: *J. Org. Chem.* **1974**, *39*, 1017.
9. *Pallas 1.2*, Prolog P software. CompuDrug Chemistry, Ltd., Budapest 1994.
10. a) Bhattacharya S., Snehalatha K.: *Langmuir* **1997**, *13*, 378; b) Burnside B. A., Knier B. L., Mackay R. A., Dupont Durst H., Longo F. R.: *J. Phys. Chem.* **1988**, *92*, 4505; c) Ghosh K. K., Satnami M. L.: *Colloids Surf., A* **2006**, *274*, 125.
11. Scrimin P., Tecilla P., Tonellato U., Bunton C. A.: *Colloids Surf., A* **1998**, *144*, 71.
12. Myers D.: *Surfaces, Interfaces, and Colloids, Principles and Applications*, pp. 333–343. VCH Publishers, Weinheim 1991.
13. Bunton C. A., Nome F. A., Quina F. H., Romsted L. S.: *Acc. Chem. Res.* **1991**, *24*, 357.

14. Mancin F., Tecilla P., Tonellato U.: *Langmuir* **2000**, *16*, 227.
15. Armarego W. L. F., Perrin D. D.: *Purification of Laboratory Chemicals*, 4th ed. Butterworth–Heinemann, Oxford 1996.
16. Gulick W. M., Jr., Geshe D. H.: *J. Am. Chem. Soc.* **1966**, *88*, 2928.
17. Merten H., Gilman H.: *J. Am. Chem. Soc.* **1954**, *76*, 5798.
18. *Origin 6.1*. OriginLab Corporation, Northampton 2000.
19. Terrier F., MacCormack P., Kizilian E., Hallé J. C., Demerseman P., Guir F., Lion C.: *J. Chem. Soc., Perkin Trans. 2* **1991**, 153.